Journal Homepage: -www.journalijar.com

INTERNATIONAL JOURNAL OF ADVANCED RESEARCH (IJAR)

ISSN NO. 2320-5407

Article DOI:10.21474/IJAR01/18009
DOI URL: http://dx.doi.org/10.21474/IJAR01/18009

*RESEARCH ARTICLE*

# NUMERICAL MODELING OF THE ASYMMETRIC HOT PLATE METHOD CONSIDERING LATERAL CONVECTIVE LOSSES

**Mohameth Dia[1], Mamadou Salif Diallo[1], Mactar Faye[1,2] and Vincent Sambou[2]**

1. Energy Efficiency and Systems Research Group, Alioune Diop University, Bambey Senegal.
2. Laboratory of Applied Energetics, Cheikh Anta Diop University, Dakar Senegal.

## Manuscript Info

*Manuscript History*
Received: 15 October 2023
Final Accepted: 18 November 2023
Published: December 2023

*Key words:-*
Asymmetric Hot Plate, Convection Coefficient, Conductivity, Diffusivity, Estimates

## Abstract

In this study, a numerical model of the asymmetric hot plate method was developed to determine the thermal properties of materials. The proposed model considers the convective heat loss around the device. First, a numerical calculation code is developed to determine the temperature evolution at the measurement points. This calculation code is then used to perform a reduced sensitivity study on various parameters. The Levenberg-Marquardt algorithm was used to identify the thermal properties of different materials from the thermogram. The impacts of the convection coefficient h and insulation thickness on the calculation of the estimates were studied. Finally, an experimental study was conducted using several materials. The thermal properties were compared with experimental results obtained using other measurement methods. A satisfactory agreement was obtained.



## Introduction:-

To reduce the energy consumption of buildings, it is imperative to develop new, more efficient materials. Adding an insulating component to a building material improves its thermal insulation properties. The use of these materials in buildings requires a thorough understanding of their thermal properties. Knowledge of these thermal properties enables modeling to predict their thermal behavior (Ma et al., 2021). In the literature, there are several measurement methods for determining the thermal properties of materials. These measurements can be carried out under steady-state or transient conditions. Steady-state measurements of thermal conductivity (Dubois & Lebeau, 2015; Zarr et al., 2017)are based on temperature differences between the heated and unheated sides. The disadvantage of steady-state measurements is that they take a very long time. Furthermore, these methods can only determine thermal conductivity. On the other hand, transient measurements (Malinarič, 2016; Malinarič & Dieška, 2020; Sabir Salim, 2022)can be used to determine at least two thermal properties. These transient methods can be applied more easily to small sample sizes, with relatively short measurement times, but have a few drawbacks. These drawbacks are often linked to assumptions and parameters not taken into account, which can limit the range of applications.

For example, the transient plane source (TPS) method (Elkholy et al., 2019)is used to determine thermal conductivity and diffusivity. The TPS method assumes that the heat flow is unidirectional (1D) at the measurement point, ignoring convective heat loss around the device. As a result, the precision of the TPS method is 2–5% for thermal conductivity, but 5–10% for thermal diffusivity. A modification of the dynamic plane source method was proposed by Malinaric et al (Malinarič et al., 2012)for characterizing low-conductivity materials. The model is

**Corresponding Author:- Mohameth Dia**
Address:- Energy Efficiency and Systems Research Group, Alioune Diop University, Bambey Senegal.

validated by comparing the results with those obtained using the TPS methodand the extended dynamic plane source method.The results show a relative error of less than 2% for thermal conductivity and 5% for thermal diffusivity.

The various methods mentioned are typically designed symmetrically, which involves the use of two perfectly identical materials. However, this requirement poses a significant challenge, as it is often extremely difficult to acquire two materials with strictly identical thermal properties and water content. In particular, obtaining identical thermal properties and similar water content for both materials can be affected by natural variations, manufacturing differences or other external factors. This inherent difficulty highlights the challenges faced by practitioners when implementing these methods, while underlining the need for alternative solutions or adaptive approaches to overcome these constraints.

It is, therefore, preferable to use methods requiring the use of a single material, such as the flash method (Laaroussi et al., 2014), the three-layer method (Jannot et al., 2009).However, the flash method is difficult to adapt to porous materials. This is because the supposedly uniform incident flux is absorbed only on the surface of the sample. Porous materials may contain air, which can interfere with the measurement of thermal conductivity by affecting heat propagation through the material. Secondly, the assumption of equal exchange coefficients between the front and back faces is contestable for a highly insulating or even super-insulating material, and separating these coefficients in the model generally leads to correlations with thermal properties that are therefore difficult to estimate separately. The three-layer method is suitable only for low-density insulating materials, and is difficult to apply to materials with high conductivity. This method leads to an accuracy of 2% for thermal conductivity estimation, taking into account the parallel resistance in the model (Bahrani et al., 2014).No validation was carried out for thermal diffusivity.

One solution is to modify the geometry of heating element methods. The hot plate method (Zhang & Degiovanni, 1993)is particularly interesting, and has been improved several times over the past few years. This method can be used to determine two thermal properties and is suitable for both thin and thick materials. Jannot et al (Jannot, Felix, et al., 2010) have used the hot plate symmetry method to characterize thin insulating materials. It has been shown that thermal conductivity can be estimated with good precision. However, the precision of the thermal capacity depends a priori on the density of the material. In addition, the thermal capacity of the sample is strongly correlated with the thermal capacity of the heating element. It has been shown that an asymmetrical device can decorrelate these two parameters. By decorrelating these two parameters, the precision of the sample's thermal capacity can be improved if the thermal capacity of the heating element is known. Bal et al (Bal et al., 2012)have used the asymmetric hot plate method with an insulated back face to characterize building materials. The proposed model allows both effusivity and thermal conductivity to be determined from a single temperature measurement. The model was validated by a comparative study with the flash methodand the mini hot plate method (Jannot, Remy, et al., 2010)on PVC material. It is shown that the difference between the estimated values and the values measured by the other two methods is less than 4%. In the hot-plate method, the precision of the thermal conductivity is very low for some material. To improve this precision, Osseni et al (Osséni et al., 2017)modified the system proposed by Bal et al (Bal et al., 2013)by introducing a second temperature measurement on the back of the sample. This thermogram can be used to improve thermal conductivity estimates.It was shown that an accurate estimation of thermal effusivity could be achieved by using the temperature of the heated face at the start of the heating process. In addition, it has been shown both theoretically and experimentally that the simultaneous use of both face temperatures improves the accuracy of thermal conductivity estimation. In some cases, particularly for low-diffusivity materials such as PVC, this approach made it possible to estimate both thermal effusivity and conductivity, when estimating thermal conductivity from the temperature of the heated face alone was not possible.A configuration of the asymmetric hotplate method has already been used previously by Jannot and al. (Jannot et al., 2006)for estimating the thermal conductivity and effusivity of high-conductivity materials. The method was tested on four metal alloys with thermal conductivities ranging from 6 to 140 $\mathrm{W\,m^{-1}K^{-1}}$with quite satisfactory results, since the average deviation from measurements made with a hot disc or a differential scanning calorimeter (DSC) was of the order of 5%.

All these asymmetrical hot plate models are based on the fundamental assumption that heat flow is unidirectional (1D). This simplifying assumption, while facilitating analysis, has significant limitations. In particular, the constraint of unidirectional heat flow restricts the ability to fully exploit the information available in the thermogram over an extended period of time. Real thermal processes can be more complex, with temporal and spatial variations that are not fully captured by a strictly unidirectional approach. Consequently, this limitation leads to reduced accuracy on one of the parameters, as the model does not adequately account for multi-dimensional variations in heat flux. It therefore becomes crucial to recognize these inherent limitations and take into account more sophisticated approaches to modeling complex thermal systems more accurately, in order to improve the accuracy of the results obtained.

The aim of this work is to develop a numerical model of the asymmetric hot plate method, taking into account convective lateral losses. The structure of this paper begins with the modeling and resolution of the system using the finite volume method (FVM) coupled with an implicit Euler scheme. Subsequently, a numerical calculation code was developed to determine the temperature evolution at the measuring point. A study of the impact of the convection coefficient on the temperature distribution was carried out. Next, a study of the reduced sensitivity of temperature to thermophysical parameters and the convection coefficient was carried out. The Levenberg-Marquardt algorithm is used to calculate the estimates. Finally, to validate the proposed model, an experimental study was carried out on a range of materials. A comparative study of the results obtained with other measurement methods was also carried out.

## Materials and Methods:-

### Mathematical modeling of the device

The heating element is inserted between the material to be characterized and a material of known thermal properties. A constant temperature is set on the back of the samples, and the system exchanges heat by convection with the surrounding environment. The proposed model is shown in Fig.1.

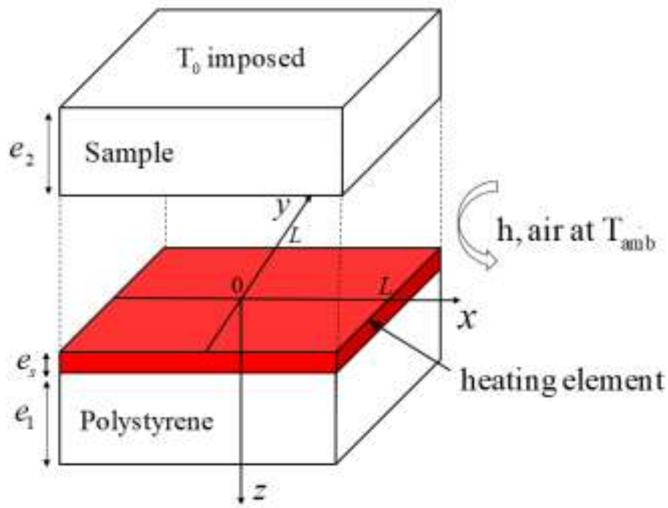


**Fig.1:-** Diagram of the proposed asymmetric model.

The mathematical model of the 3D heat conduction in the transient regime applicable to each material is expressed as follows :

$$\nabla.\left(\lambda\nabla T\right)dVdt = \rho c\frac{\partial T}{\partial t}dVdt \quad \in \ \Omega \quad (1)$$

The initial condition can be written as :

$$\left\{at \quad t=0 \quad T(x,y,z,0) = T_0 \right. \quad \in \ \Omega \quad (2)$$

The boundary conditions on the lateral surfaces of the device are identical (convection), so to save computation time we have modeled the ¼ of the device shown inFig.1. The boundary conditions at x = 0 ; y = 0 are written as follows :

$$\begin{cases} at\ x=0 & \dfrac{\partial T(0,y,z,t)}{\partial x} = 0 \\ at\ y=0 & \dfrac{\partial T(x,0,z,t)}{\partial y} = 0 \end{cases} \quad \in \ \Gamma_1 \ (3)$$

The lateral convective losses can be taken into account in a simple way with the assumption that the temperature and convection coefficient are uniformaround the device. The heat transfer boundary condition is given by :

$$\begin{cases} at\ x = L & -\lambda \dfrac{\partial T(L,y,z,t)}{\partial x} = h\left[ (T((L,y,z,t)) - T_{amb}) \right] \\ at\ y = L & -\lambda \dfrac{\partial T(x,L,z,t)}{\partial y} = h\left[ (T((x,L,z,t)) - T_{amb}) \right] \end{cases} \quad \in \ \Gamma_2 \tag{4}$$

Where λis the thermal conductivity of the sample ($Wm^{-1}K^{-1}$). The thermal diffusivity ($m^2/s$) is given by $a = \lambda/\rho c$ and ρ, c represents respectively the density ($kgm^{-3}$) and the specific heat ($Jkg^{-1}K^{-1}$). We consider $e_1$ , $e_2$and $e_s$ as the thickness of theinsulator, the sampleand the heating element respectively. The temperature on the back side of the sample is $T_0$ and his the convection coefficient of convective heat transfer ($Wm^{-2}K^{-1}$) supposed to be uniform along the walls. T is the temperature of the material $T_{amb}$ is the temperature of the environment. And $\Gamma_1$ is the symmetry condition, $\Gamma_2$ is the Fourier boundary condition, and Ω is the entire model area.The integration of Equation (1) on a control volume C allows us to determine its integral balance form :

$$\iint_{V_C} \nabla.\left(\lambda \nabla T\right) dVdt = \iint_{V_C} \left(\rho c\right) \times \frac{\partial T}{\partial t} dVdt \tag{5}$$

The divergence theorem allows us to rewrite equation (5) as follows :

$$\int_{S_C} \lambda \nabla T \times dSdt = \int \left(\rho c\right) V_C \times \frac{\partial T}{\partial t} dt \tag{6}$$

Equation (6)becomes :

$$\sum_{F \in NB(C)} \lambda \left(\nabla T\right)_F \times S_F = \int \left(\rho c\right) V_C \times \frac{\partial T}{\partial t} dt \tag{7}$$

Assuming that the discretization domain is uniform, the step length in the x-axis is $\Delta x = x_{i+1} - x_i$ ; along the y-axis is $\Delta y = y_{i+1} - y_i$ ; and along the z-axis is$\Delta z = z_{i+1} - z_i$. The variable n ($n$ = 0, 1, 2, 3 . . .) is used to uniformly discretize the time domain for $t \geq 0$and the length of the steps between two temporal moments $\Delta t = t_{n+1} - t_n$ .For a regular structured grid, each interior node of the domain is connected to the same number of neighboring nodes.These neighboring cells can be identified by indices i, j and k in the directions of the x, y and z coordinates, respectively, and can be accessed directly by incrementing or decrementing the respective indice.Assuming a linear variation of T, the x, y, z component of the gradient can be written as follows :

$$\begin{aligned} \left(\nabla T\right)_E &= \frac{T_E - T_C}{\Delta x} \quad ; \quad \left(\nabla T\right)_W = \frac{T_C - T_W}{\Delta x} \\ \left(\nabla T\right)_T &= \frac{T_T - T_C}{\Delta z} \quad ; \quad \left(\nabla T\right)_B = \frac{T_C - T_B}{\Delta z} \\ \left(\nabla T\right)_N &= \frac{T_N - T_C}{\Delta y} \quad ; \quad \left(\nabla T\right)_S = \frac{T_C - T_S}{\Delta y} \end{aligned} \tag{8}$$

Time discretization is performed using the implicit Euler scheme. The advantage of adopting an implicit scheme is that it is unconditionally stable.

$$\left(\frac{\partial T}{\partial t}\right) = \frac{T_C^n - T_C^{n-1}}{\Delta t} \tag{9}$$

Applying equation (9) and equation (8) to equation (7) gives the following temperature expression at node C :

$$\begin{aligned} &\left[ \left(\rho c\right) \frac{\Delta x \Delta y \Delta z}{\Delta t} + 2\frac{\lambda\, \Delta y \Delta z}{\Delta x} + 2\frac{\lambda\, \Delta x \Delta z}{\Delta y} + 2\frac{\lambda\, \Delta x \Delta y}{\Delta z} \right] T_C^n = \frac{\lambda\, \Delta y \Delta z}{\Delta x}\left(T_E^n - T_W^n\right) \\ &+ \frac{\lambda\, \Delta x \Delta z}{\Delta y}\left(T_N^n - T_S^n\right) + \frac{\lambda\, \Delta x \Delta y}{\Delta z}\left(T_T^n - T_B^n\right) + \left(\rho c\right)\frac{\Delta x \Delta y \Delta z}{\Delta t} T_C^{n-1} \end{aligned} \tag{10}$$

Where :

$T_C^n$ : temperature of central node C at time t.
$T_C^{n-1}$ : temperature of central node C at time t–Δt.
$T_N^n$; $T_S^n$; $T_B^n$; $T_T^n$; $T_E^n$; $T_W^n$ : temperature of neighboring nodes.
To reduce calculation time, an additional hypothesis has been made, considering that heat transfer occurs along the (Ox) and (Oz) axes. With this hypothesis, the temperature $T(x_i, z_k, t_n)$depends only on x and z, so equation (10) becomes :

$$\left[(\rho c)\frac{\Delta x\Delta y\Delta z}{\Delta t}+2\frac{\lambda\,\Delta y\Delta z}{\Delta x}+2\frac{\lambda\,\Delta x\Delta y}{\Delta z}\right]T_C^n=\frac{\lambda\,\Delta y\Delta z}{\Delta x}\left(T_E^n-T_W^n\right)+\frac{\lambda\,\Delta x\Delta y}{\Delta z}\left(T_T^n-T_B^n\right)+(\rho c)\frac{\Delta x\Delta y\Delta z}{\Delta t}T_C^{n-1} \tag{11}$$

Boundary conditions at measurement point x = 0 ; z=0 :

- Symmetry conditions :

$$\left\{\frac{\partial T_W^n(0,0,t)}{\partial x}=0\right. \tag{12}$$

- The contact thermal resistance Rc between the heating element and the sample at the measurement point is defined as :

$$\left\{-\lambda\frac{\partial T_C^n\left(0,0,t\right)}{\partial z}=\frac{T_C^n\left(0,0,t\right)-T_N^n\left(0,z,t\right)}{R_C}\right. \tag{13}$$

Applying equations (13) and (12) to the equation (11), we determine the temperature evolution at the measuring point as follows :

$$\left[(\rho c)_S\frac{\Delta x\Delta z}{\Delta t}+\frac{\lambda_s\Delta z}{\Delta x}+\frac{\lambda_s\Delta x}{\Delta z}+\frac{\Delta x}{R_C}\right]T_C^n=\frac{\lambda_s\Delta z}{\Delta x}T_E^n+\frac{\lambda_s\Delta x}{\Delta z}T_B^n+\frac{\Delta x}{R_C}T_N^n+(\rho c)_S\frac{\Delta x\Delta z}{\Delta t}T_C^{n-1} \tag{14}$$

Where $\lambda_S$is the thermal conductivity of the heating element ($Wm^{-1}K^{-1}$) ;ρ, c represents respectively the density ($kgm^{-3}$) and the specific heat ($Jkg^{-1}K^{-1}$) of the heating element.

**Description of the experimental approach formeasurements**

A MINCO HR5178 R42.9L heating element, consisting of a nickel spiral with layers of kapton on either side, is connected to a current generator (TTI, PL330, 32V-3A, PSU) to apply heat flux to the sample.A type K thermocouple, made of chromel and alumel with a diameter of 0.03 mm, is connected to an acquisition unit (Picolog-TC-08) to measure temperature evolution.A material with known thermal properties (e.g. polystyrene) is placed on the bottom of the heating element, and the sample to be characterized is placed on the top. The materials, heating element and aluminum blocks have the same dimensions, i.e. 10x10 cm. Once the experimental temperature has stabilized, i.e. when the ambient temperature, the temperature at the center of the heating element and the temperature at the back of the sample differ by a maximum of 1%, the current in the heat source is activated and simultaneously the acquisition unit starts recording temperatures.

A clamping device is used to join the materials together. It should be noted that the mechanical pressure exerted by the clamping device could affect the contact resistance. As the model is asymmetrical, it generates two contact resistances, $R_{C_1}$ and $R_{C_2}$. To neglect $R_{C_2}$, we used a deformable insulating material with a thickness of up to 5 cm. To minimize contact resistance, thicknesses were selected so that the ratio $e/_{\lambda}$was greater than 0.01 (Jannot, Remy, et al., 2010). For example, for a material with conductivity $\lambda = 0.032\,Wm^{-1}K^{-1}$ and a thickness of 5 cm, the thermal resistance of the sample is given by $e/_{\lambda} = 0.64\,KW^{-1}m^{-2}$. Thus, contact thermal resistances can be neglected in relation to the thermal resistance of the sample. The temperature $T_C$ was measured by a K-type thermocouple inserted inside the heating element to limit the contact thermal resistance $R_{C_1}$.

The features described above are illustrated inFig.2, which shows the version of the experimental set–up used for the measurements described in this article.The thermal properties of the materials described in Fig.2 are reported in

Table 1. It should be pointed out that the thermal properties of the heating element are not perfectly known, so we assume its thermal properties.

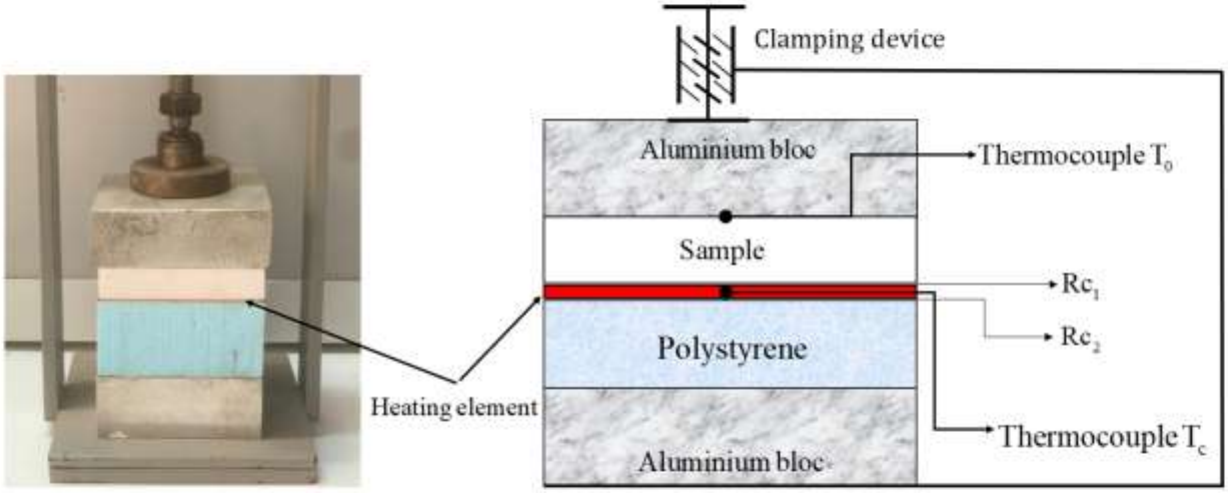


**Fig.2:-** View and schema of the experimental device.

The temperature in the aluminum blocks is assumed to be uniform(Jannot, Felix, et al., 2010).It turns out that the temperature $T_0(e_2, t)$increases after a certain time corresponding to the long time (Fig.3 ; Fig.4). This temperature can be consideredconstant,as the maximum deviation between $T_0(e_2, 0)$and$T_0(e_2, t_f)$ is less than 1%.Fig.3and Fig.4also show temperature versus time for the 2D model developed in Matlab and the 3D model simulated in COMSOL. The study shows that the 2D model perfectly represents the 3D model for an exchange coefficient $h = 10\ Wm^{-2}K^{-1}$. The mean deviation between the 3D and 2D models is less than 1%, which is quite satisfying. Therefore, this 2D model can be used to perform the estimations.

**Table 1:-** Thermal properties of materials used in simulation.

| Materials | $\lambda\ (Wm^{-1}K^{-1})$ | $\rho c(Jm^{-3}K^{-1})$ | $a\ (m^2s^{-1})$ | e (cm) |
|---|---|---|---|---|
| Heating element | 0.3 | 1200000 | $2.5 \times 10^{-7}$ | $2.2\times 10^{-2}$ |
| Polystyrene | 0.032 | 48000 | $6.6667\times 10^{-7}$ | 5 |
| Laterite | 0.5 | 930000 | $5.3763\times 10^{-7}$ | 3 |
| Vermiculite | 0.08 | 160000 | $5.00\times 10^{-7}$ | 3 |

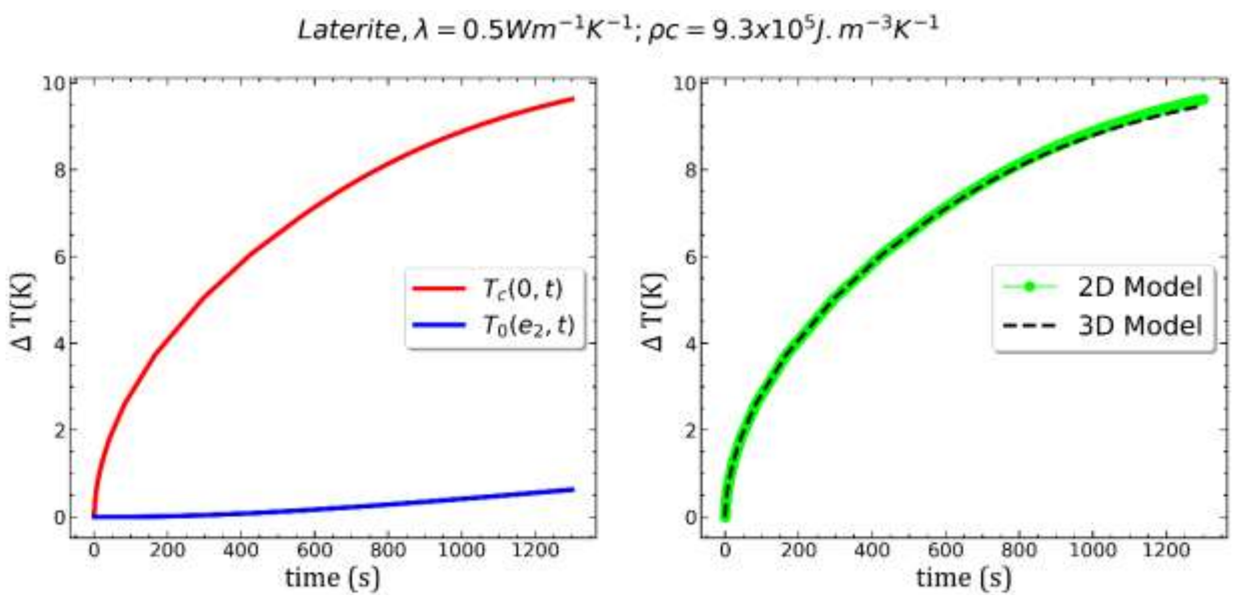


**Fig.3:-** Evolution of temperatures on both sides of the sample as well as the 2D and 3D model.

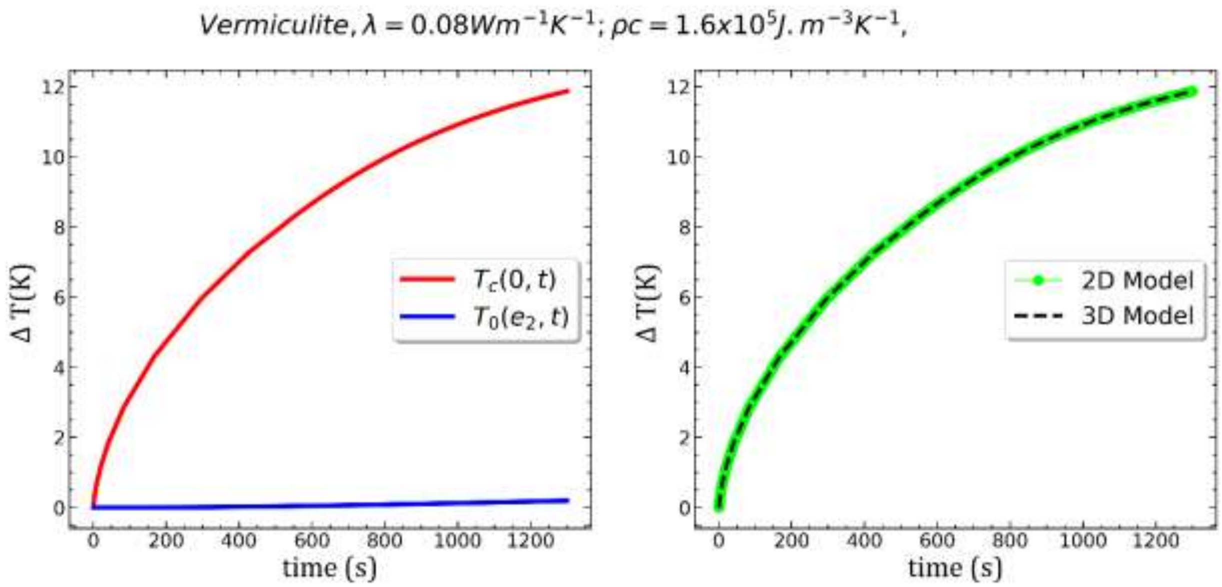


**Fig.4:-** Evolution of temperatures on both sides of the sample as well as the 2D and 3D model.

**Temperature distribution across the material**

The 3D model (Fig.1) is based on the assumption that the horizontal end surfaces of the device ($\Gamma_3$) are maintained at a uniform and constant temperature. The vertical sides of the zone ($\Gamma_2$) are in contact with the ambient air with a uniform surface heat transfer coefficient by natural convection, h. The vertical sides of the zone ($\Gamma_1$) are considered adiabatic conditions for symmetry reasons. The three-dimensional transient heat conduction Eq.(1) is applicable to all layers of the model. The calculations were performed using the COMSOL Multiphysics finite element software. Rectangular meshes of 120 x 120 were used in the (x, y) planes, and along the z-axis the number of mesh $M_z$is given in Table 2along with the thermal properties of the materials.

**Table 2:-** Parameters of simulation.

| Materials | $\lambda\ (Wm^{-1}K^{-1})$ | $\rho c(Jm^{-3}K^{-1})$ | $a\ (m^2s^{-1})$ | e (cm) | $M_z$ |
|---|---|---|---|---|---|
| Heating element | 0.3 | 1200000 | $2.5\times10^{-7}$ | $2.6\times10^{-2}$ | 10 |
| Laterite | 0.5 | 930000 | $5.3763\times10^{-7}$ | 3 | 60 |
| Polystyrene | 0.032 | 48000 | $6.6667\times10^{-7}$ | 3 | 60 |

The objective of these simulations is to study the impact of the convective flow on the temperature distribution in any region (Ω) in particular at the heating element. For this purpose, two values of the convective coefficient were considered :$h = 0\ Wm^{-2}K^{-1}$ et $h = 10\ Wm^{-2}K^{-1}$. The former allows the model to be simulated in the absence of convective flow on the vertical sides of the $\Gamma_2$ zone.

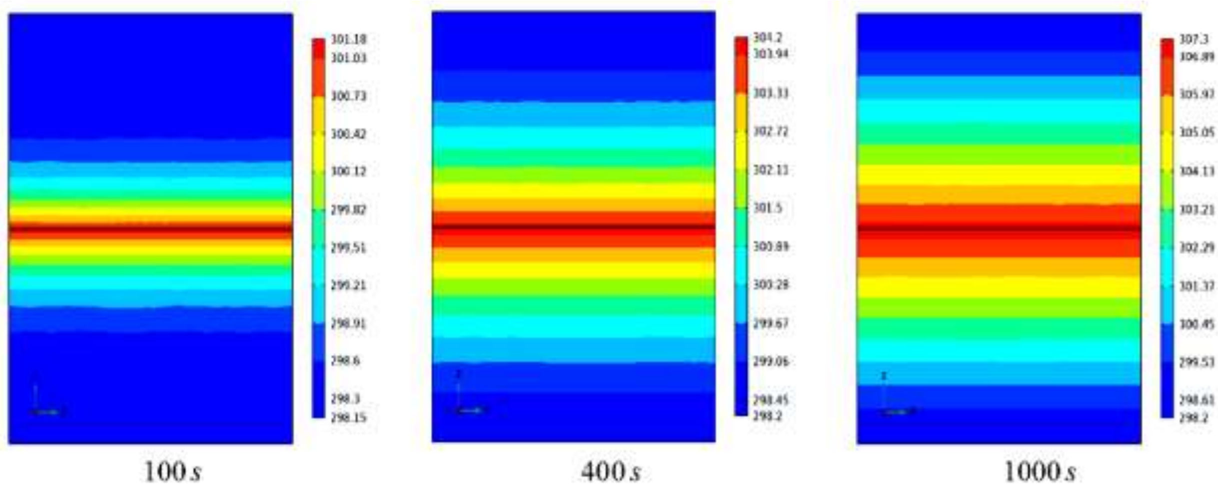


**Fig.5:-** Temperature distribution on the yz plane for $\mathbf{h = 0\ Wm^{-2}K^{-1}}$

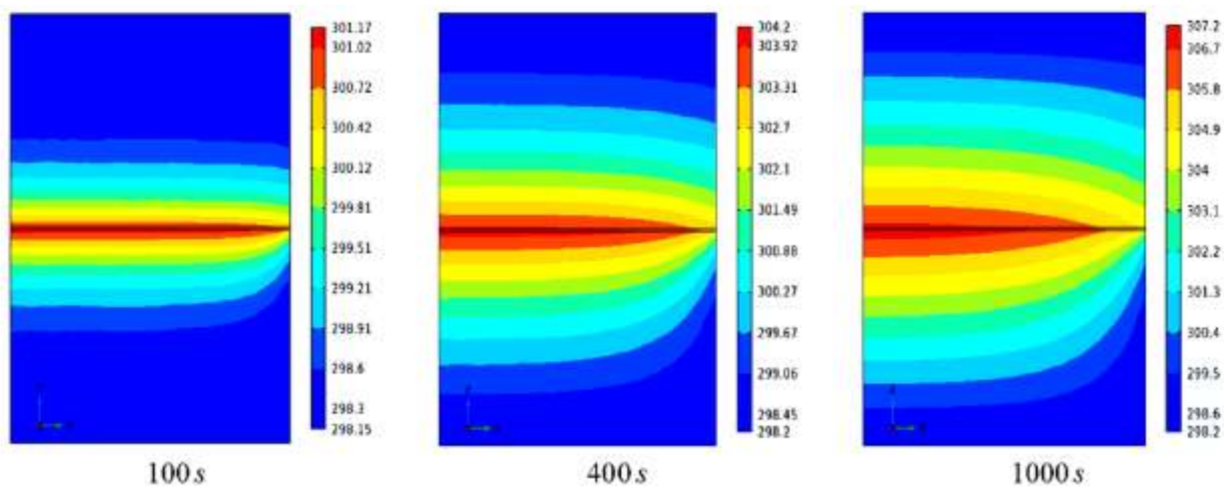


**Fig.6:-** Temperature distribution on the yz plane for $\mathbf{h = 10\ Wm^{-2}K^{-1}}$

Fig.5shows the temperature distributions on the (y, z) plane for different time intervals. This study shows that there is no deviation of the isothermal lines, the temperature is uniform along the x–axis. The second one allows the simulation of the model in the presence of the convective flow over the $\Gamma_2$ zone (Fig.6). As expected, this study shows a deviation of the isothermal lines on the walls. As the heating time increases, this disturbance increases around the location of the thermocouple (measurement point). Thus, the direction of the heat flow is no longer unidirectional (1D), unlike the previous case.

**Reduced sensitivity analysis**

A reduced sensitivity analysis is performed to determine if the parameters λ, a, Rc, and h are estimable. Using the 2D calculation code developed in Matlab, this analysis can be performed using relation(15):

$$X_i\left(t, B\right) = B_i\ \frac{\partial T}{\partial B_i} \tag{15}$$

Where$B_i$ is the parameter to be estimated.The sensitivity analysis was performed for PVCmaterial whose thermal properties are reported in theTable 3.The results are shown in Fig.7.

**Table 3:-** Values of the thermal properties.

| | $\lambda$ $(Wm^{-1}K^{-1})$ | ρc $(Jm^{-3}K^{-1})$ | $a$ $(m^2s^{-1})$ | e (cm) |
|---|---|---|---|---|
| Insulation | 0.032 | 48000 | $6.667 \times 10^{-7}$ | 4 |

| | | | | |
|---|---|---|---|---|
| PVC | 0.187 | 1375200 | $1.362\times 10^{-7}$ | 1.5 |

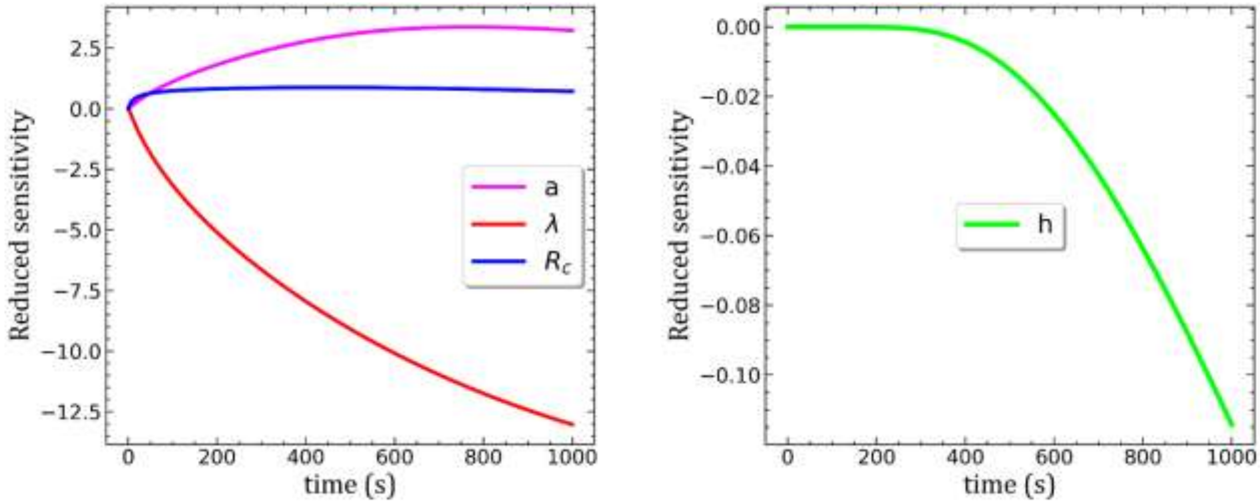


**Fig.7:-** Reduced sensitivity of the PVC material.

Fig. 7 shows that the exchange coefficient only becomes sensitive after 300s for the PVC material. This observation can also be explained by the fact that lateral losses take time to become apparent at the measurement point, as shown in the previous study. In addition, it is highly decorrelated from the other parameters, so it will be possible to estimate it. It can also be seen that the reduced sensitivity of thermal conductivity is very important, as is the sensitivity of thermal diffusivity. The contact resistance Rc is sensitive at the start of the experiment and then remains constant. For simultaneous estimation of these parameters to be possible, they must be linearly unrelated. The sensitivities of a, λ, and Rc are decorrelated, as shown in Fig.8. It appears that the convection coefficient is decorrelated from the other parameters.Simultaneous estimation of these parameters will be possible.

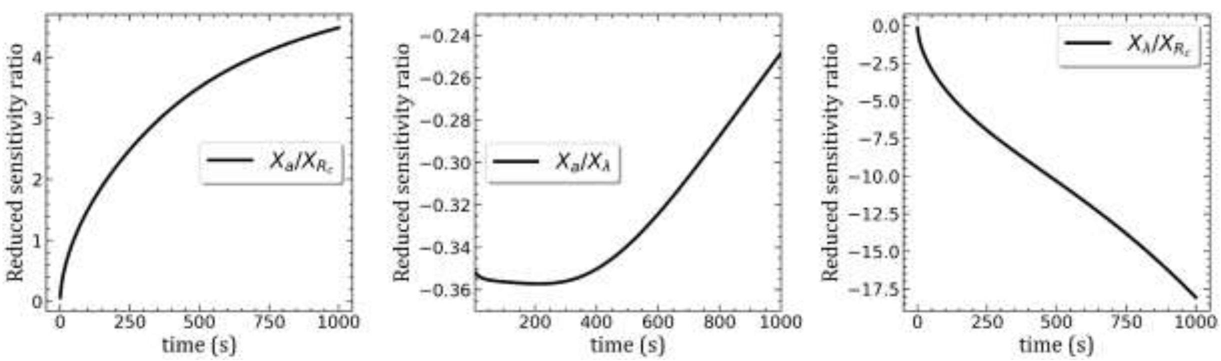


**Fig.8:-** Reduced sensitivity ratio of parameters a, λ and Rc for the PVC material.

## Results and Discussion:-

### Insulation optimization

The aim of the following estimations is to identify an optimum insulation thickness range. To this end, thermograms for the various materials (Table 4) are simulated with insulation thickness values ranging from 1 to 5 cm. The thermal properties of the insulation are :$\lambda = 0.0302\ Wm^{-1}K^{-1}$ ; $\rho c = 48000\ Jm^{-3}K^{-1}$.White noise of zero mean and standard deviation $\sigma_{bruit} = 0.02K$ is added to the simulated data to give it an experimental character. The standard deviations of estimates for each parameter are shown as a function of insulation thickness in the Fig.9.

**Table 4:-** Thermal properties of some materials.

| | $\lambda\ (Wm^{-1}K^{-1})$ | $a\ (m^2s^{-1})$ | $\rho c\ (Jm^{-3}K^{-1})$ | $\Phi\ (Wm^{-2})$ | e (cm) |
|---|---|---|---|---|---|
| Clay brick | 1.15 | 7.2766 x $10^{-7}$ | 1.5804 x $10^{6}$ | 450 | 3 |
| Laterite | 0.5 | 5.3763 x $10^{-7}$ | 9.3 x $10^{5}$ | 200 | 3 |

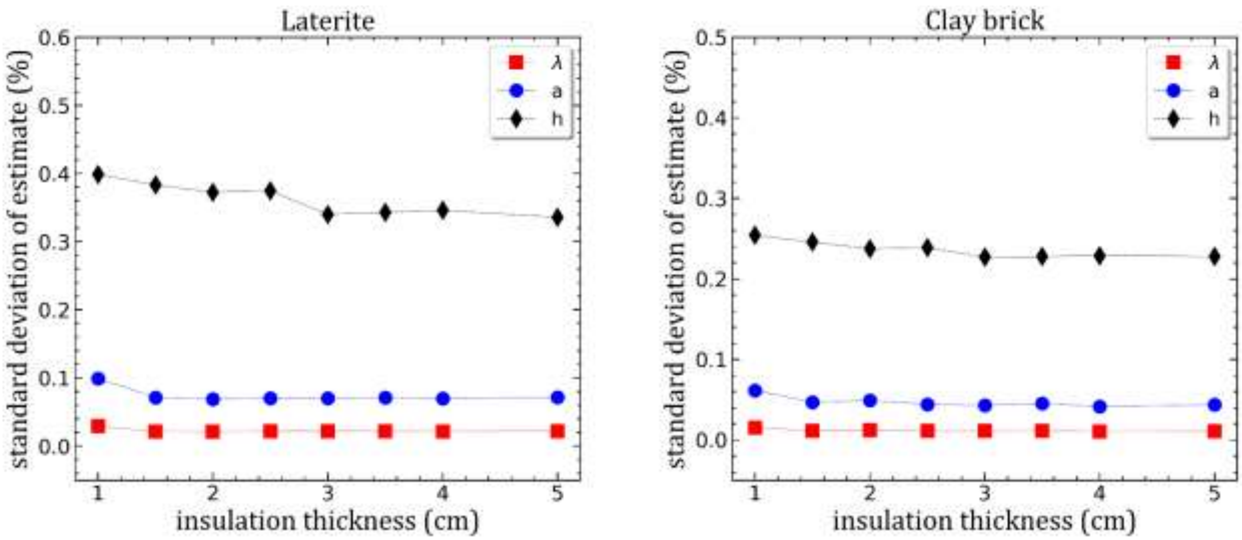


**Fig.9:-** Estimation of thermophysical parameters as a function of insulation thickness.

The results in Fig.9show that the choice of insulation thickness does not affect estimates of thermal conductivity, thermal diffusivity and convection coefficient. These thermal parameters remain relatively stable despite variation in insulation thickness, as the analysis of the results clearly shows. This finding suggests that, for the purposes of this study, the 4 cm thickness of polystyrene might be an appropriate option.

**Effect of convection coefficient on estimates**

In practice, it is difficult to estimate the heat transfer coefficient h with precision.In this section, we will evaluate the uncertainties caused by this parameter in the estimation of λ and a. For different values of the convection coefficient h ranging from (2 – 15) $Wm^{-2}K^{-1}$, the thermal conductivity and diffusivity were estimated. The estimated values were compared with their reference value given in Table 4 (Clay Brick). Fig.10shows the relative errors in thermal conductivity and diffusivity as a function of the value of the convection coefficient h.

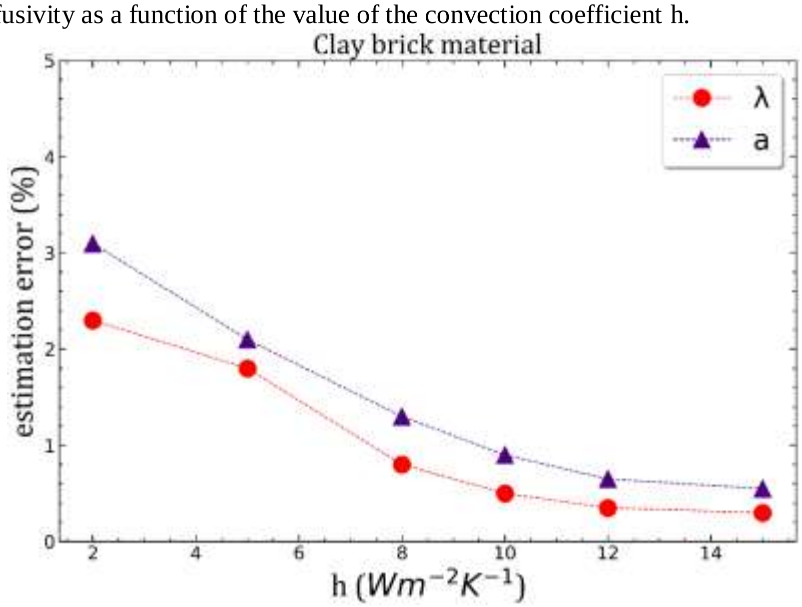


**Fig.10:-** Estimation of thermal conductivity and diffusivity for different values of the convection coefficient h.

Fig.10shows that for h = $2Wm^{-2}K^{-1}$the relative error on thermal diffusivity can be slightly over 3%. However, it can be seen that the higher the value of the convection coefficient, the lower the corresponding error on thermal conductivity and diffusivity. It should be noted that these estimates were made assuming perfect contact between the heating element and the sample. This assumption can be justified by the thermal accommodation criterion, which is less than 0.1. As a result, the heat flux through the samples increases, and heat losses decrease.

## Experimental Results and Discussion:-

In our model, the heat flux density is expressed as a function of the thermal resistance $R_{el}$, the surface area S of the heating element and the electric current I by the following equation.

$$\varphi_0 = \frac{R_{el}}{S} I^2 \tag{16}$$

In practice, we set a voltage U(V) and then measure the current I(A)delivered by the generator. The hot plate method is not absolute, requiring an extension to determine the $\frac{Rel}{S}$ ratio. After calibration tests, the results showing that the ratio $\frac{Rel}{S} = 3986.9\ \Omega m^{-2}$can be considered.Uncertainty in the surface area of the heating element, the thickness of the sample and the heat flux produced by the heating element lead to an overall uncertainty of 3.6%. These uncertainties were calculated in our previous work(Dia et al., 2023).Experimental measurements were carried out on several different materials :

- M1 :wood-based material, 1.8 cm thick.
- M2 :PVC-based material, 1.5 cm thick.
- M3 :Polystyrene-based material, 2.2 cm thick.
- M4 :PVC-based material, 2 cm thick.

The thermal conductivity of M1 measured by the hot wire method (Assael et al., 2008)is$0.134\ Wm^{-1}K^{-1}$, the thermal effusivity is measured by the asymmetric hot plate method $354\ Jm^{-2}K^{-1}s^{-\frac{1}{2}}$which leads to a thermal diffusivity of $1.4329 \times 10^{-7} m^2 s^{-1}$. Thermal properties of M2 given by the asymmetric hot plate method (Bal et al., 2013)are : $\lambda = 0.182\ Wm^{-1}K^{-1}$ ; $a = 1.362 \times 10^{-7} m^2 s^{-1}$ ; forM3 : $\lambda = 0.0305\ Wm^{-1}K^{-1}$ ;$a = 2.231 \times 10^{-6} m^2 s^{-1}$ ;forM4 : $\lambda = 0.103\ Wm^{-1}K^{-1}$ ;$a = 2.281 \times 10^{-7} m^2 s^{-1}$.Three measurements were performed for each sample to estimate the measurement errors. The values of the parameters λ, a, Rc, and h were estimated by minimizing the sum of the squared deviations $\psi = \sum_{j=0}^{N} \left[T_{exp}(t_j) - T_{mod}(t_j)\right]^2$between the experimental curve$T_{exp}(t)$and the theoretical curve $T_{mod}(t)$calculated by the relation(14).The minimization of the sum is performed using the Levenberg–Marquardt algorithm.Thermal capacity can be deduced from conductivity and thermal diffusivity.Fig.11shows an example of experimental and theoretical curves with estimated parameters and residuals.

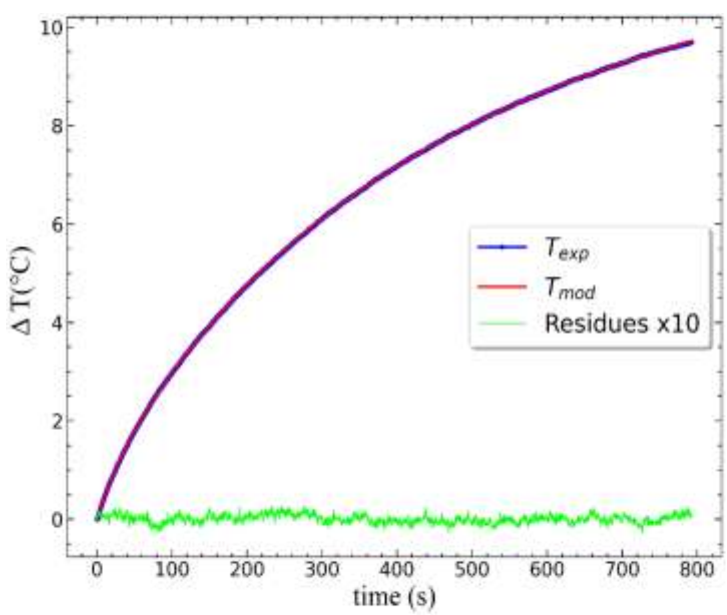


**Fig.11:-**Experimental and theoretical curve, estimation residuals x10.

Fig.11shows that the theoretical curve obtained by relation (14) and the experimental curve are perfectly superposed. Residuals are flat and centered on 0, indicating an absence of model bias. Table 5 presents a synthesis of the experimental results.

**Table 5:-** Results of the estimations.

| Test Nr | Material | $\frac{\lambda}{Wm^{-1}K^{-1}}$ | $\frac{a}{(m^2s^{-1})}$ | $\frac{\rho c}{Jm^{-3}K^{-1}}$ | $\frac{h}{Wm^{-2}K^{-1}}$ | $\frac{Rc}{m^2KW^{-1}}$ | $\frac{Residus}{\sigma_{res}(\%)}$ |
|---|---|---|---|---|---|---|---|
| 1er | M1 | 0.139 | $1.525\times 10^{-7}$ | 911480 | 5.128 | 0.0012 | 0.0104 |
| 2er | | 0.139 | $1.504\times 10^{-7}$ | 924200 | 5.771 | 0.0012 | 0.0101 |
| 3er | | 0.137 | $1.499\times 10^{-7}$ | 913940 | 5.019 | 0.00115 | 0.0095 |
| Mean | | **0.138** | $\mathbf{1.509\times 10^{-7}}$ | **916540** | **5.3060** | **0.0012** | |
| Standard deviation | | **0.835 %** | **0.914 %** | **0.736 %** | **7.658%** | | |
| 1er | M2 | 0.186 | $1.358\times 10^{-7}$ | 1369700 | 5.452 | 0.0009 | 0.008 |
| 2er | | 0.188 | $1.351\times 10^{-7}$ | 1391600 | 5.037 | 0.0015 | 0.008 |
| 3er | | 0.188 | $1.377\times 10^{-7}$ | 1365300 | 4.658 | 0.0015 | 0.013 |
| Mean | | **0.187** | $\mathbf{1.362\times 10^{-7}}$ | **1375500** | **5.0490** | **0.0013** | |
| Standard deviation | | **0.617 %** | **0.988 %** | **1.024 %** | **7.865%** | | |
| 1er | M3 | 0.0309 | $2.446\times 10^{-6}$ | 12633 | 5.124 | 0.00032 | 0.0102 |
| 2er | | 0.0315 | $2.257\times 10^{-6}$ | 13957 | 5.165 | 0.00021 | 0.0138 |
| 3er | | 0.0312 | $2.311\times 10^{-6}$ | 13501 | 5.168 | 0.00032 | 0.0107 |
| Mean | | **0.03120** | **2.338**$\times 10^{-6}$ | **13364** | **5.1523** | **0.00028** | |
| Standard deviation | | **0.962 %** | **4.164 %** | **5.033 %** | **0.477 %** | | |
| 1er | M4 | 0.1013 | $2.277\times 10^{-7}$ | 444880 | 5.535 | $4.86\times 10^{-5}$ | 0.023 |
| 2er | | 0.1010 | $2.441\times 10^{-7}$ | 413760 | 5.626 | $4.66\times 10^{-5}$ | 0.024 |
| 3er | | 0.1012 | $2.367\times 10^{-7}$ | 427550 | 6.089 | $5.55\times 10^{-5}$ | 0.023 |
| Mean | | **0.1012** | $\mathbf{2.362\times 10^{-7}}$ | **428730** | **5.7497** | $\mathbf{5.0233\times 10^{-5}}$ | |
| Standard deviation | | **0.151 %** | **3.478 %** | **3.637 %** | **5.171 %** | | |

The results show :

1. the estimated values of the thermal conductivity λ of the different materials are in good agreement with those measured using the hot wire and hot plate methods (relative deviation less than 3%). The standard deviation of the measurements was compared with the mean value, leading to a standard deviation of less than 1% between the three experimental tests.The thermal conductivities of these materials were estimated with high reproducibility.These results demonstrate excellent precision and reproducibility in estimating the thermal conductivities of these materials.
2. the thermal diffusivity was obtained from the thermal effusivity using the hot-plate method. The values measured using this method were very close (relative deviation less than 5%).For materials M1 and M2, the standard deviation of the measurements between the three experimental tests was less than 1 %.We can conclude that for heavy materials, the thermal diffusivity of these materials can be estimated with high reproducibility.
3. For the estimation of the convection coefficient (h), the value obtained is in the range associated with natural convection. However, the standard deviation of the measurement exceeds 5% for materials M1, M2 and M4. This higher variability is explained by the low sensitivity of the convection coefficient to these materials, hindering more accurate estimation. In addition, it should be noted that the convection coefficient (h) is temperature-dependent, which can introduce variations. Consequently, consistency and uniformity are not guaranteed after each measurement, contributing to the complexity of estimating the convection coefficient under these conditions.

## Conclusion:-

Asymmetrical hot-plate methods are based on the assumption of unidirectional (1D) heat flow at the point of measurement. However, this assumption limits the exploitation of the thermogram over a sufficiently long period of time to obtain greater accuracy in the estimation of thermophysical parameters. This work aims to eliminate this limitation by taking into account lateral convection losses around the device. For this purpose, the proposed model was first solved using the finite volume method (FVM) associated with an implicit Euler scheme. The 2D

calculation code, developed in Matlab, was validated by comparing the results of the 2D model with those of the full 3D model simulated in COMSOL Multiphysics. The results show perfect agreement between the two models, suggesting that the 2D model is suitable for making the estimates.Next, a reduced sensitivity study was carried out to evaluate the identifiability of the thermophysical parameters. The results confirm that these parameters are estimable. The impact of insulation thickness and exchange coefficient h on the estimates was studied. The conclusions show that the choice of insulation thickness does not significantly affect the estimates. However, for an exchange coefficient $h = 2\ Wm^{-2}K^{-1}$, a slight error of over 3% is observed on thermal diffusivity.
Finally, an experimental study was carried out on several materials. Estimates showed good agreement with other measurement methods. Analysis of the standard deviations of the measurements reveals that the experiment is reproducible for the determination of thermal conductivity and diffusivity. However, it should be noted that the thermal resistance between the material of known thermal property and the heating element was neglected. In addition, the convection coefficient is a parameter dependent on ambient temperature. Despite these additional considerations, the experimental results show a relative error of around 3% for conductivity and 5% for thermal diffusivity. These deviations remain within acceptable limits, underlining the overall robustness of our experimental approach.

**Declaration of competing interest**
The authors have no conflictsto disclose.

**Data access statement**
The data that support the findings of this study are available from the corresponding author upon reasonable request.

## References:-


1. Assael, M. J., Antoniadis, K. D., Kakosimos, K. E., & Metaxa, I. N. (2008). An Improved Application of the Transient Hot-Wire Technique for the Absolute Accurate Measurement of the Thermal Conductivity of Pyroceram 9606 up to 420 K. International Journal of Thermophysics, 29(2), 445-456. https://doi.org/10.1007/s10765-007-0333-5
2. Bahrani, S. A., Jannot, Y., & Degiovanni, A. (2014). Extension and optimization of a three-layer method for the estimation of thermal conductivity of super-insulating materials. Journal of Applied Physics, 116(14), 143509. https://doi.org/10.1063/1.4897507
3. Bal, H., Jannot, Y., Gaye, S., & Demeurie, F. (2013). Measurement and modelisation of the thermal conductivity of a wet composite porous medium : Laterite based bricks with millet waste additive. Construction and Building Materials, 41, 586-593. https://doi.org/10.1016/j.conbuildmat.2012.12.032
4. Bal, H., Jannot, Y., Quenette, N., Chenu, A., & Gaye, S. (2012). Water content dependence of the porosity, density and thermal capacity of laterite based bricks with millet waste additive. Construction and Building Materials, 31, 144-150. https://doi.org/10.1016/j.conbuildmat.2011.12.063
5. Dia, M., Faye, M., Diallo, M. S., & Sambou, V. (2023). Measurement of the thermal properties of materials by the hot plate method considering the convection coefficient around the device. Materials Research Express, 10(6), 065502. https://doi.org/10.1088/2053-1591/acdce4
6. Dubois, S., &Lebeau, F. (2015). Design, construction and validation of a guarded hot plate apparatus for thermal conductivity measurement of high thickness crop-based specimens. Materials and Structures, 48(1-2), 407-421. https://doi.org/10.1617/s11527-013-0192-4
7. Elkholy, A., Sadek, H., & Kempers, R. (2019). An improved transient plane source technique and methodology for measuring the thermal properties of anisotropic materials. International Journal of Thermal Sciences, 135, 362-374. https://doi.org/10.1016/j.ijthermalsci.2018.09.021
8. Jannot, Y., Acem, Z., & Kanmogne, A. (2006). Transient hot plate method with two temperature measurements for thermal characterization of metals. Measurement Science and Technology, 17(1), 69-74. https://doi.org/10.1088/0957-0233/17/1/012
9. Jannot, Y., Degiovanni, A., & Payet, G. (2009). Thermal conductivity measurement of insulating materials with a three layers device. International Journal of Heat and Mass Transfer, 52(5-6), 1105-1111. https://doi.org/10.1016/j.ijheatmasstransfer.2008.09.017
10. Jannot, Y., Felix, V., & Degiovanni, A. (2010). A centered hot plate method for measurement of thermal properties of thin insulating materials. Measurement Science and Technology, 21(3), 035106. https://doi.org/10.1088/0957-0233/21/3/035106
11. Jannot, Y., Remy, B., & Degiovanni, A. (2010). Measurement of thermal conductivity and thermal resistance with a tiny hot plate. High Temperatures-High Pressures, 39, 11-31.

12. Laaroussi, N., Lauriat, G., Garoum, M., Cherki, A., & Jannot, Y. (2014). Measurement of thermal properties of brick materials based on clay mixtures. Construction and Building Materials, 70, 351-361. https://doi.org/10.1016/j.conbuildmat.2014.07.104
13. Ma, A., Cai, C., Yang, J., & Zhou, T. (2021). Measuring thermophysical properties of building insulation materials using transient plane heat source method. Energy and Buildings, 240, 110891. https://doi.org/10.1016/j.enbuild.2021.110891
14. Malinarič, S. (2016). Step-wise transient method. Measurement Science and Technology, 27(3), 035601. https://doi.org/10.1088/0957-0233/27/3/035601
15. Malinarič, S., & Dieška, P. (2020). New evaluation of the step-wise transient measurements. 020019. https://doi.org/10.1063/5.0025894
16. Malinarič, S., Dieška, P., & Krupa, P. (2012). Modified Dynamic Plane Source Method for Measuring Thermophysical Parameters of Solids. International Journal of Thermophysics, 33(3), 528-539. https://doi.org/10.1007/s10765-012-1173-5
17. Osséni, S. O. G., Ahouannou, C., Sanya, E. A., & Jannot, Y. (2017). Hot Plate Method with Two Simultaneous Temperature Measurements for Thermal Characterization of Building Materials. International Journal of Thermophysics, 38(6), 81. https://doi.org/10.1007/s10765-017-2217-7
18. Sabir Salim. (2022). Thermal conductivity measurements using the transient hot-wire method : A review— IOPscience. https://iopscience.iop.org/article/10.1088/1361-6501/ac90df
19. Zarr, R. R., Guthrie, W. F., Hay, B., & Koenen, A. (2017). Collaborative guarded-hot-plate tests between the Laboratoire national de métrologie et d'essais and the National Institute of Standards and Technology. Metrologia, 54(1), 113-128. https://doi.org/10.1088/1681-7575/aa4e55
20. Zhang, X. X., & Degiovanni, A. (1993). Mesure de l'effusivité thermique de matériaux solides et homogènes par une méthode de "sonde" plane. Journal de Physique III, 3(6), 1243-1265. https://doi.org/10.1051/jp3:1993196.